

# Andosols of the Bambouto Mountains (West Cameroon): Characteristics, Superficial Properties - Study of the Phosphate Ions Adsorption

Siéwé Jean Mermoz<sup>a</sup>, Djoufac Woumfo Emmanuel<sup>\*a</sup>, Bitom Dieudonné<sup>b</sup>, Figueras François<sup>c</sup>, Djomgoué Paul<sup>a</sup>, Njopwouo Daniel<sup>a</sup> and Azinwi Primus Tamfuh<sup>b</sup>

<sup>a</sup>Laboratoire de Physico-chimie des Matériaux Minéraux, Faculté des Sciences, Université de Yaoundé I B.P. 812 Yaoundé, Cameroun

<sup>b</sup>Laboratoire de Pédologie, Faculté des Sciences, Université de Yaoundé I B.P. 812 Yaoundé, Cameroun

<sup>c</sup>IRCELYON, UMR 5256, CNRS-Université LYON 1, 2, Avenue A. Einstein, 69626 Villeurbanne, France

**Abstract:** The present work is focussed on the characterisation and the study of the surface properties of the Mount Bambouto andosols in view of their use in the adsorption of phosphate ions. The particle size distribution analysis has revealed a low clay content (9 %) meanwhile the silt content is high (70 %). Some surface properties like zero point charge (4.4), cationic exchange capacity (32.2 meq/100g), surface area (50.12 m<sup>2</sup>/g) of the material were measured. The adsorption kinetics of the phosphate ions is of second order. The removal of organic matter using hydrogen peroxide aqueous solutions enables to increase the quantity of the adsorbed phosphate ions at pH 6.6 from 4.15 mg/g to 6.10 mg/g. Minerals with hydroxyl groups like allophane, gibbsite and goethite are responsible for the phosphate ions adsorption but these hydroxyl groups are destroyed in acidic medium. The raw andosol adsorbs much more phosphate ions than its fine fraction (0-2 µm) because of the destruction of the allophane – humus complex during various extraction operations (crushing and dispersing).

**Keywords:** Bambouto mountains, andosol, allophane, superficial properties, adsorption, phosphate.

## 1. INTRODUCTION

The main regions of the world that favour the formation and the conservation of andosols are those of recent volcanic activity outstandingly Japan, New Zealand, America (The Andes mountain range), France (Massif central), Cameroon (Mount Cameroon, Bambouto mountains), the Antilles...[1-4]. The works of Tematio *et al.* [3] and Tematio [4] in the Mount Bambouto situated in West Cameroon (Central Africa), have revealed the presence of organic matter-rich (8-23 %) andosols in the upper part of the massif that extends between 2000 and 2740 m altitude. This zone is marked by a fresh, humid (2510 mm of rainfall/year) and cloudy climate. The soils are characterized by a thick humiferous horizon (>60 cm) that shows a very dark brown colour, high porosity and an unctuous touch when humid. The mineralogy is marked by the presence of halloysites, gibbsite, goethite and amorphous minerals such as allophane and ferrihydrite. Those short-ranged allophane minerals are noticeable by their very high specific area (370-670 m<sup>2</sup>/g) according to Diez *et al.* [5], their vital role in soil fertilization [6] and their phosphate adsorptive properties [7].

Excess phosphates derived from fertilizers and detergents can end up in lakes and rivers thus promoting the development of aquatic plants like algae. Such plants prevent the penetration of sunlight and oxygen which causes eutrophica-

tion. Much work has already been consecrated to phosphate removal making use of several methods which can be biological, or chemical treatment with aluminum, iron and calcium precipitation. These methods are ineffective at low concentration [8]; the adsorption of phosphate ions at the surfaces of materials, like clays, has been rather recommended for low concentrations [9-11]. It depends on the presence of some minerals like goethite, gibbsite, allophane and it is generally attributed to the presence of iron and aluminum hydroxides (Fe-OH and Al-OH) at the surfaces of these minerals [11,12]. This adsorption, according to Ho *et al.* [13], Eun Woo *et al.* [8] Banat *et al.* [14] can either be by chemisorption or by physical adsorption.

The aim of this paper is to study phosphate ions adsorption on Bambouto's andosols in relation with some characteristics like particle size distribution, specific surface and porosity, organic matter, mineralogy, and pH. The sorption mechanisms of phosphate ions shall be determined.

## 2. MATERIAL AND EXPERIMENTAL METHODOLOGY

### 2.1. Material

The material examined in this study is an andosol collection that was sampled on the southern flank of Mount Meletan at the summit of the Bambouto massif (West Cameroon in Central Africa) between 2000 and 2740 m altitude. The Bambouto massif is an enormous volcanic shield located on the Cameroon volcanic line (latitude 5°30' – 5°50' N, longitude 9°93' - 10°13' E). The sample was collected in the humiferous layer of the profile (0-60 cm) [4]. It is dark brown

\*Address correspondence to this author at the Laboratoire de Physico-chimie des Matériaux Minéraux, Faculté des Sciences, Université de Yaoundé I B.P. 812 Yaoundé, Cameroun; E-mail: edjoufac2000@yahoo.fr

in color, has a  $\text{pH}_{\text{H}_2\text{O}}$  of 5.2, a real density of 2.4, a silty texture and a lumpy structure. The material is very porous, friable and fragile with the presence of gramineae roots [4]. The samples were air-dried in the laboratory to a constant weight before grinding and sieving in a 160  $\mu\text{m}$  diameter seave.

## 2.2. Experimental Methodology

### 2.2.1. Particle Size Distribution and Sample Pre-Treatment

The particle size distribution analysis was done by sieving method for particle diameters above 100  $\mu\text{m}$  and by sedimentometry for diameters below 100  $\mu\text{m}$  [15]. 1000 g of the material that has been dried to constant weight was collected and immersed in water for 24 h before it was allowed to pass through a 5, 2, 1, 0.63, 0.1, mm sifter column. After successive rinsing, the collected refuse was collected and oven-dried at 105 °C for 24 h. It was then allowed to cool before weighing. The < 100  $\mu\text{m}$  fraction was used for particle size distribution analysis by settling; it enables to determine the percentage of clay (0- 2  $\mu\text{m}$ ), silty (0-50  $\mu\text{m}$ ) and sandy (>50  $\mu\text{m}$ ) fractions.

The various clay and clay-silty fractions were obtained by sedimentation of a previously crushed raw andosol material which was dispersed in a 1 %  $\text{Na}_2\text{CO}_3$  solution according to stokes law in an Atterberg cylinder. The clay fraction denoted FF (0 – 2  $\mu\text{m}$ ) was siphoned after 7 h of settling; the clay-silty fraction denoted ZV (0-20  $\mu\text{m}$ ) after 4 min [15]. The different fractions obtained were air-dried at 28-30 °C.

The elimination of the amorphous minerals was done according to the method proposed by Segalen [16]. The amorphous silica was removed by reacting 0.5 g of the material with 50 ml of a 0.5 N NaOH solution in a water bath at 80 °C for 30 min. The amorphous alumina contained in 0.5 g material was eliminated by treatment with 50 ml of an 8 N HCl solution over 30 min.

Two methods were used to eliminate the organic matter, viz the thermal method at 350 °C during 4 h (for the Ad-350 sample) and the treatment with a 10 % hydrogen peroxide aqueous solution (for the Ad- $\text{H}_2\text{O}_2$  sample).

### 2.2.2. Sample Characterization

The major elements of the Ad-brut sample were titrated using atomic absorption spectrometry (AAS) at the “Centre de Recherche Pétrographique et Géologique (CRPG) de Nancy (France)” after melting of the samples with  $\text{LiBO}_2$  and dissolving in nitric acid. The results were expressed in terms of % of the most stable oxides.

The XRD analysis on powder sample was performed with a Sigma 2080 Diffractometer using a Cu anticathode with a counting speed of 0.022° per 34.5 s between 5 and 70°.

Thermal gravimetric analysis (TGA) and its derivative (DGTA) were done under standard conditions using a SETARAM TGDTA92 apparatus.

The specific area and the porosity of the material have been determined by the BET method in the “Laboratoire de Physique - Chimie et Microbiologie pour l’Environnement” of the Henri Poincaré University, Nancy, France.

The determination of the zero point charge (ZPC) was done by potentiometric method [17].

The cationic exchange capacity (CEC) was measured by the  $\text{H}^+$  ions method in the form of a resin H [18].

### 2.2.3. Adsorption and Dosage of Phosphate Ions

100 ml of a standard solution of phosphate ions were placed in a 250 ml beaker. The required acidic or basic pH was readjusted using an HCl or NaOH solution. 1 g of the andosol material was then added and the mixture was stirred for 15 min and allowed to rest for 24 h. After centrifugation, the phosphate ions were titrated by the colorimetric method of Rodier [19]. The absorbance of the filtrate was read using a HITACHI U-2000 spectrophotometer with a wavelength of 700 nm. To minimize manipulation errors, a phosphate reference solution was measured against the phosphate adsorbing sample.

## 2.3. Phosphate Adsorption Model

Many publications [20, 21] have revealed that the adsorption model of phosphate ions on the surface of andosols generally agrees with the Langmuir model; it is therefore this isotherm which was used for data analyses. The Langmuir isotherm equation is as follows:

$$Q_{\text{ad}} = \frac{K Q_{\text{max}} C_e}{1 + K C_e} \quad (1)$$

where  $Q_{\text{ad}}$  is the quantity of phosphate adsorbed at equilibrium (mg/g),  $K$  the Langmuir constant (L/g),  $Q_{\text{max}}$  the adsorption capacity (mg/g) and  $C_e$  the phosphate concentration at equilibrium.

A certain number of models are available for the kinetics of adsorption process. Those models have been used so as to determine the sorption mechanism which can either be chemisorption or physical adsorption.

The simplest model is the first order kinetics whose equation is as follows:

$$\frac{dq}{dt} = K_1 (q - q(t)) \quad (2)$$

The integration of equation (2) gives:

$$\ln\left(\frac{q - q(t)}{q}\right) = -K_1 t \quad (3)$$

Equation (3) can be written as:  $\ln(q - q(t)) = -K_1 t + \ln(q)$  (4)

where  $q(t)$  and  $q$ , in mg/g, are respectively the quantities of phosphate adsorbed at a time  $t$  (min) and at equilibrium;  $K_1$  is the constant of the first order adsorption rate. The graph of  $\ln(q - q(t))$  versus  $t$  enables to deduce  $K_1$  which is the slope of the curve.

The other sorption kinetics model is pseudo-second order, which can be expressed in differential form as:

$$\frac{dq}{dt} = K_2 (q - q(t))^2 \quad (5)$$

$$\text{This, upon integrating gives } \frac{1}{q - q(t)} = \frac{1}{q} - K_2 t \quad (6)$$

where  $K_2$  is the second order adsorption rate constant of sorption.

Equation (6) can thus be written as:

$$\frac{t}{q(t)} = \frac{1}{K_2 q^2} + \frac{1}{q} t \quad (7)$$

The rate constant  $K_2$  is obtained experimentally by plotting the curve  $t/q(t)$  versus  $t$  which gives a straight line graph with intercept of  $1/(K_2 q^2)$  and the slope  $1/q$ .

### 3. RESULTS AND DISCUSSION

#### 3.1. Particle Size Distribution Analysis

The results of the particle size distribution analysis, represented on Fig. (1), reveal 9 % clay fraction, 70 % of silt (fine and coarse silt) and 21 % of sand-sized fraction.

The particle size distribution analyses permitted us to work out the statistical distribution of spherical equivalent diameters of particles of the material [7]. In the case of the studied material, Fig. (1) displays the distribution curve of the 0-100  $\mu\text{m}$  fraction of the raw material Ad-brut; the mean equivalent diameter ( $d_{50}$ ) which is the diameter in which the statistical population is divided into two classes of equal frequencies:  $d_{50}$  is equal to 55  $\mu\text{m}$ . The dispersion interval that portrays the slanting of the particle distribution curve

$d_{75} - d_{25}$  equals 84  $\mu\text{m}$  ( $d_{75} - d_{25} = 94 - 10 = 84 \mu\text{m}$ ) and shows that the material is constituted by different aggregates.

#### 3.2. Chemical Analysis

##### 3.2.1. Major Elements

The results of the chemical analyses of major elements are assembled in Table 1.

These results reveal that the material is characterised by:

- $\text{SiO}_2/\text{Al}_2\text{O}_3 > 1$  (that is 2.45); this ratio is often encountered in andosols that are quite rich in silico-alumina amorphous products [22]. This value is however higher than that reported in silico-alumina amorphous products (0.5 and 1.8) of the andosols of Mount Cameroon [2]; this difference might be explained by the presence of quartz and feldspars that were not eliminated before the analysis;
- an  $\text{Fe}_2\text{O}_3$  content of 10.493 %, high (more than a hundred folds), compared to values documented by Mackenzie [23] for the allophane-rich soils of New Zealand. The high contents of the oxide led one to suggest the presence of amorphous or crystalline iron oxides which are the commonest minerals in andosols [2].
- equivalent  $\text{K}_2\text{O}$  and  $\text{Na}_2\text{O}$  contents (<1 %), but low concentration could be explained by the intense lixiviation of these exchangeable cations;
- low  $\text{CaO}$  (0.359 %) and  $\text{MgO}$  (0.531 %) contents which might probably portray the absence of carbon-

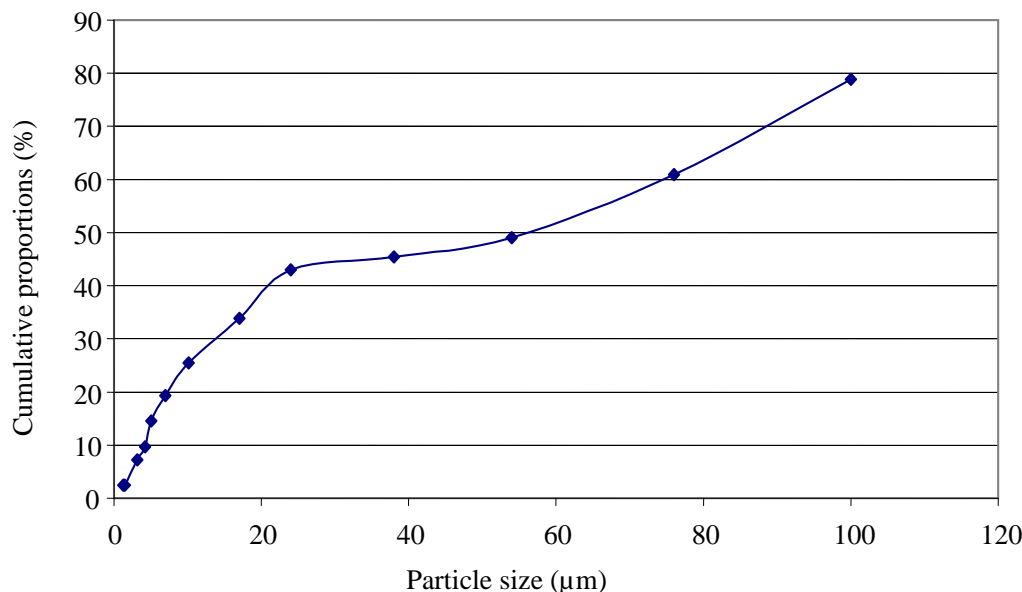


Fig. (1). Particle size distribution curve of (0- 100  $\mu\text{m}$ ) Ad-brut fraction.

Table 1. Major Elements Contents (%)

$\text{SiO}_2$	$\text{Al}_2\text{O}_3$	$\text{Fe}_2\text{O}_3$	MnO	MgO	CaO	$\text{Na}_2\text{O}$	$\text{K}_2\text{O}$	$\text{TiO}_2$	$\text{P}_2\text{O}_5$	L.I.	Total
32.468	22.537	10.493	0.21	0.531	0.359	0.114	0.423	1.704	0.419	30.287	99.525

L.I. = Loss by Ignition.

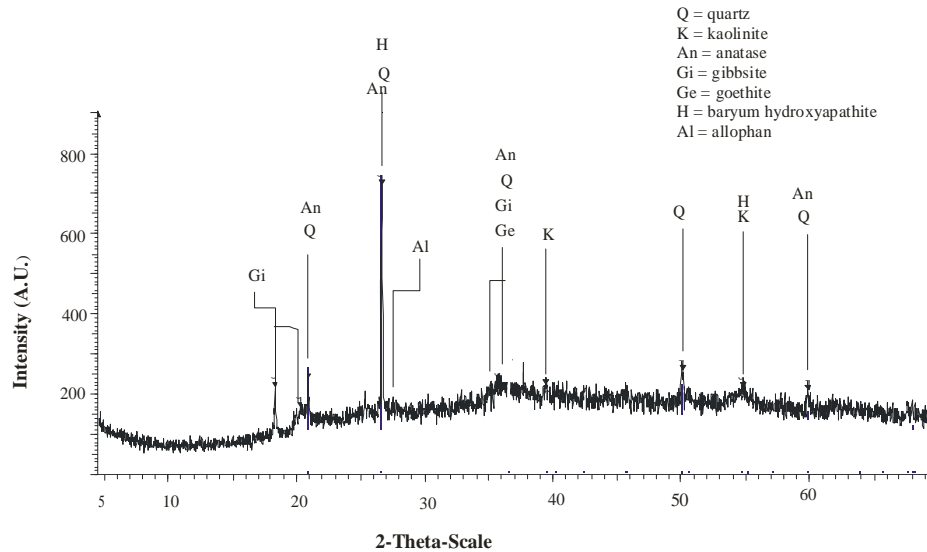


Fig. 2 X-ray diffractogram of Ad-brut

Fig. (2). X-ray diffractogram of Ad-brut.

ates in the studied material, but also the non-formation of calcium and magnesium silicates and the intense lixiviation [24];

- a high loss on ignition, > 30 %, which is an evidence of the low clay mineral contents in the andosols [25] and might also imply the presence of water and organic matter in the material. From the real density values ( $Dr = 2.4$ ) recorded by Tematio [4], the organic matter contents (O.M.), were deduced from the Pauwel's equation [29].  $Dr = 2.65 - 0.02 (\% \text{ O.M.})$ , where 2.65 is the density of quartz, meanwhile the organic matter content of the material is 12.5 %.

### 3.3. Mineralogical Analysis

The results of the x-ray diffractograms shown on Fig. (2) enabled us to identify the following minerals: kaolinite,

quartz, goethite, gibbsite, allophan, barium hydroxyapatite, and anatase. Those minerals had previously been identified by Tematio [4].

### 3.4. Thermal Analysis

The TGA and DTG curves (Fig. (3)) present two endothermic peaks which respectively slant between 0 and 180 °C for the first and between 200 and 350 °C for the second; two thermal accidents are also observable at 360 °C and 570 °C.

The first endothermic phenomenon might correspond either to the loss of hydration water of some amorphous gels (silica, aluminum hydroxide) and to the dehydroxylation of allophan [26]; the second endothermic signal can be attributed to a cristobalite-gibbsite mixture, because cristobalite that is frequent in andosols [27], presents an endothermic

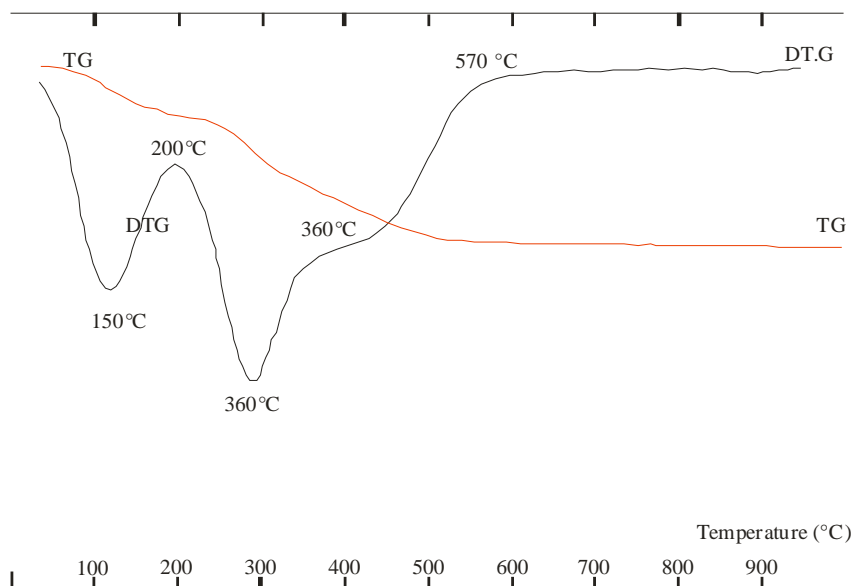


Fig. (3). Thermoanalytical curves of Ad-brut sample.

**Table 2. Specific Surface Area and Total Pore Volume**

Fraction	Ad-brut	FF	ZV
Specific surface area (m <sup>2</sup> /g)	50.12	38.89	31.04
Total pore volume (mL/g)	0.083	0.082	0.073

peak between 220 and 260 °C [28]. Gibbsite instead shows a meaningful endothermic signal between 300 and 400 °C. At 360 °C there is a small peak which can be attributed to aluminous goethite; between 370 and 570 °C, an important exothermic peak is identifiable which is characteristic of the air burning of organic matter (previously determined at more than 12 % weight of the total material), which further deforms the endothermic peak characteristic of 1:1 minerals that possibly appear between 500 and 700 °C. The thermal accidents at 570 °C and around 900 °C signal the presence of 1:1 minerals.

### 3.5. Superficial Properties

#### 3.5.1. Specific Surface and Porosity

The specific surface and the total volume of pores are represented on Table 2. The results reveal that the raw sample (Ad-brut) has the highest specific surface (50.12 m<sup>2</sup>/g) followed by the fine clay fraction (FF) (38.1 m<sup>2</sup>/g) and finally the silty clay fraction (ZV), (31.04 m<sup>2</sup>/g). The total volume of pores evolves in the same trend: 0.083 mL/g for the Ad-brut, 0.082 mL/g for FF and 0.073 mL/g for ZV.

The specific areas of the different materials presented above, range between 30 and 50 m<sup>2</sup>/g. These values are higher than those of kaolinite (10-20 m<sup>2</sup>/g) [29,30], but lower than those of allophane (1000 m<sup>2</sup>/g) as reported by Egashire

*et al.* [31] and 530 m<sup>2</sup>/g according to Hashizume *et al.* [32]. The specific area of a composite material should be dependent on the overall constituent of the material; the low specific area values shown in Table 2 might be due to the low allophane content associated to organic matter. According to Jarvinen *et al.* [33] and Chiou *et al.* [34], the specific area that has been measured by nitrogen adsorption has a negative correlation with the organic matter contents, for Ad-brut has high organic matter content (12.5 %). This might explain the low values observed. Meanwhile the specific surface has a positive correlation with the clay content [35], whereas the grain size distribution analysis has revealed relatively low clay content (9 %).

Considering the mean dimensions of allophane particles (diameter between 3.5 and 5 nm), one would have expected the fine clay (0-2 µm) fraction to be richer in allophane and hence a higher specific surface. Instead, the specific area of the raw material is higher than that of the fine clay fraction; this implies that the allophane which is the highest contributor to the specific area is more concentrated in the raw material (Ad-brut) than in the fine clay material (FF).

#### 3.5.2. Zero Point Charge

The ZPC of the raw material (Ad-brut) is equal to 4.4; this means that the surface will be positive for pH < ZPC but negative for pH > ZPC. This ZPC value is located within the

**Table 3. Comparison of Some Characteristics of the Andosols from the Bambouto Mountains to those of others Andosols Identified in the World**

Origin	SiO <sub>2</sub> /Al <sub>2</sub> O <sub>3</sub>	CEC (méq/100g)	Z PC	Loss by Ignition (%)	Specific Area (m <sup>2</sup> /g)	References
Bambouto (Cameroun)	2.45	32	4.4	30	50.12	/
Azores (Portugal)	/	21.8	4.1	/	/	[36]
New Zealand	(1 – 2)	/	5.7	/	537	[32]
Kitakami	1.47	43	/	/	/	[26]
Choyo (Japan)	1.99	118	/	/	/	
Nyanget (Finland)	/	17.00	5.1	/	160	[37]
Derbyshire (England)	0.93	/	/	37	/	[23]
Silica Springs (New Zealand)	1.15	/	/	40.50	/	[23]
Hyytiala (Finland)	/	5.11	4.41	/	73.7	[37]
Azores (Portugal)	/	17.4	4.1	/	/	[36]
Iwat (Japan)	1.30	/	/	36.41	/	[23]
Kumamoto (Japan)	1.73	/	/	35.49	/	[23]

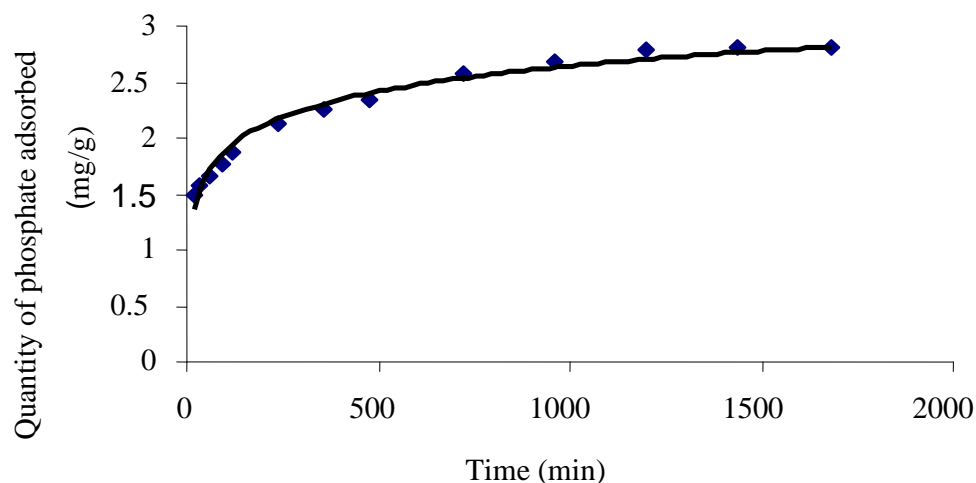


Fig. (4). Adsorption kinetics of phosphate on Ad-brut.

mean of ZPC of fundamental minerals (kaolinite, goethite, gibbsite and allophane) that ranges between 3 and 6.

### 3.5.3. Cationic Exchange Capacity

The cationic exchange capacity of the raw andosols which has been measured by resin method in a resin/clay mass ratio of 1 is equal to  $32.2 (\pm 0.1)$  meq/100g. This value agrees with the interval of literature values for andosols (20 - 45 meq/100 g) [4]. The relatively high nature of this value might be due to the presence of organic matter which amplifies the negative character of the surfaces and contributes to CEC increase [7].

### 3.6. Comparison of some Characteristics of the Bambouto's Andosols and those of other Regions in the World

A comparison of the andosols from Bambouto mountain with some andosols identified in the world (Table 3), gives the following results:

- the molar ratio  $\text{SiO}_2/\text{Al}_2\text{O}_3$  which is equal to 2.45, is higher than other reported ratios found in the world,

this could be explained by the presence of quartz and feldspars;

- the CEC of the samples presented in Table 3 varies from 5 to 118 meq/100g. It seems to be proportional to the allophane rate present in the material;
- the ZPC which is equal to 4.4, is in the interval of the values documented by Madeira *et al.* [36] for the andosols of Azores (Portugal) and also with those found by Karlum *et al.* [37] for the andosols of Hyytiala (Finland). This value is lower than 5.7, found by Hahizumę *et al.* [32] for an andosol sample from New Zealand;
- the loss on ignition 30.11 % remains characteristic of the andosols such as those studied by Mackenzie [23] out of two andosols samples from England;
- the specific area of Mount Bambouto's raw sample which is equal to 50.12 m<sup>2</sup>/g, is lower than that found by Hahizumę *et al.* [32] on andosols from New Zealand (537 m<sup>2</sup>/g) and also than a Finnish sample (160 m<sup>2</sup>/g) found by Karlum *et al.* [37]. However, another

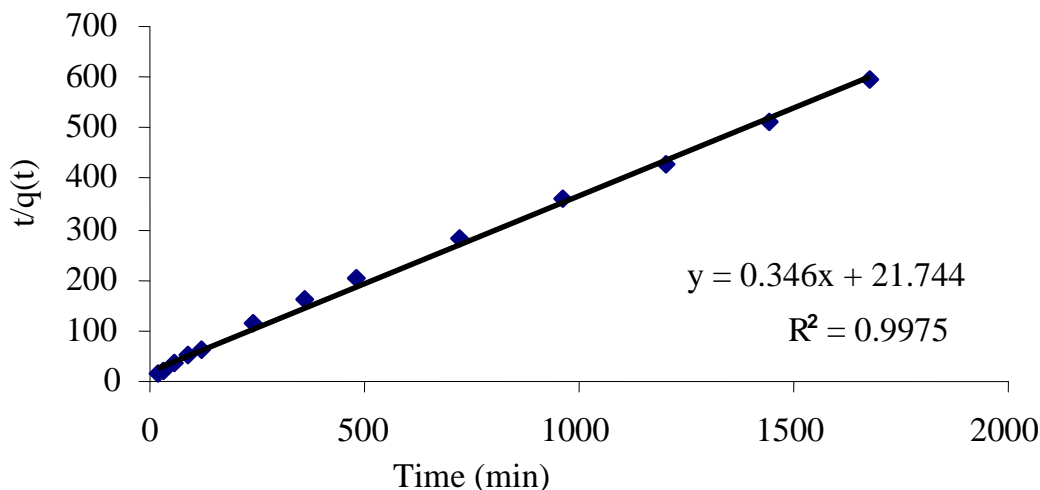


Fig. (5). Representation of the kinetics data by the second-order model (Eq. (7))

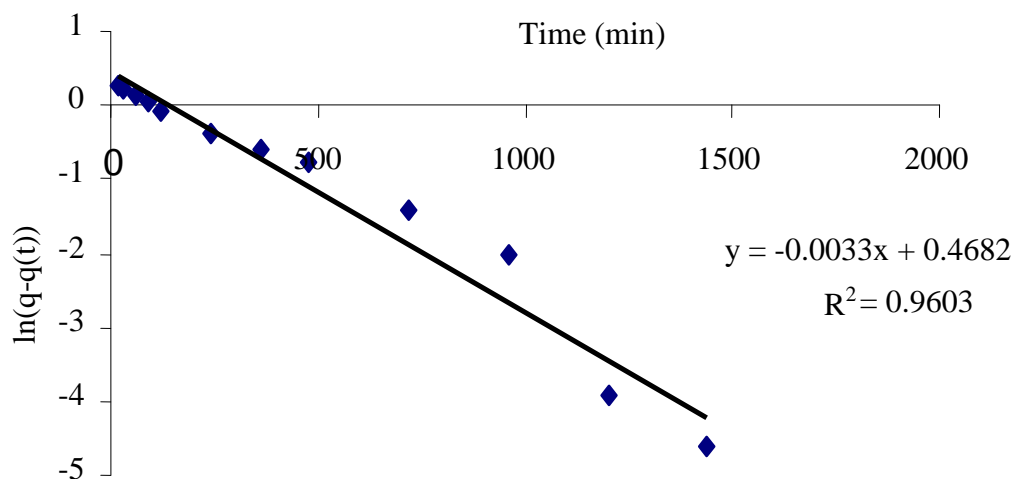


Fig. (6). Representation of the kinetics data by the first-order model (Eq. (4)).

Finnish sample [37] with 73.7 m<sup>2</sup>/g of specific area is rather close to the values reported in the Bamboutou mountains.

### 3.7. Phosphate Adsorption

#### 3.7.1. Adsorption Kinetics

Fig. (4) shows the quantity of phosphate ions in mg/g adsorbed with respect to time at 30 °C. It is observed here that the maximum adsorption value is practically attained after 20 h of contact. The plotted curve shows that the adsorption of phosphate ions is done in two steps: a rapid step that proceeds within 2 h 30 min during which 1.87 mg of phosphate ions are adsorbed by 1g of andosols, and a second step which is slower and which portrays a progressive evolution towards equilibrium. During this second step, 0.94 mg of phosphate ions are adsorbed by 1g of andosols for a duration of 21 h 30 min. Gilles *et al.* [38], Torrent *et al.* [39] and Barrow *et al.* [40] refer this slow evolution towards equilibrium to the diffusion of the adsorbed molecules into the micropores of the andosols.

In order to determine the order of the phosphate ions adsorption reaction on the andosols surface, the data on kinetic study were analysed according to the linear shapes of equations (4) and (5) and the results obtained are presented on Fig. (5) and (6). The determination of the coefficients of correlation ( $R^2$ ) for the first order models gives 0.9603 while that of the second order gave 0.9975 which expresses in a better way the order of the reaction; this reaction is a chemisorption process.

#### 3.7.2. Influence of Mineralogy on Phosphate Ion Adsorption

The phosphate ion adsorption capacity (0.06 mg/g for Ad-(X-OH) against 3.08 mg/g for Ad-brut) shows a reduc-

tion of more than 88 %. Table 4 shows that Ad-(X-OH) which was previously treated with an 8 N HCl and 0.5 N NaOH solutions almost shows no phosphate adsorptive capacity relative to the raw andosols (Ad-brut). This is certainly due to the fact that the 8 N HCl solution and 0.5 N NaOH solutions have destroyed the minerals responsible for adsorption of the phosphate ions notably allophane.

Table 4. Quantity of Phosphate Adsorbed by Ad-brut and Ad-(X-OH)

Material	Ad-brut	Ad-(X-OH)
Quantity of phosphate adsorbed (mg/g)	3.08	0.06

#### 3.7.3. Influence of Particle Size Distribution on Phosphate Ion Adsorption

Table 5 is a representation of the quantity of phosphate ions adsorbed relative to the various fractions at 30 °C. 1 g of raw andosols practically adsorbs twice that adsorbed by 1 g of the fine clay fraction. It is noted that the maximum quantity adsorbed per gram obeys the following order: Ad-brut > FF > ZF. This trend is identical to that of the specific surface and porosity of these fractions. This observation therefore confirms the presence of a greater amount of allophane in the raw andosol material. One could believe that the various operations such as crushing and dispersion lead to the destruction of the allophane-humus complex. This explains why the raw andosol has a higher specific surface compared to the clay and silty clay fractions.

#### 3.7.4. Influence of Organic Matter

The influence of organic matter has been studied according to two methods: a chemical treatment with hydrogen peroxide aqueous solution (Ad-H<sub>2</sub>O<sub>2</sub>) and a thermal treat-

Table 5. Influence of Particle Size Distribution on Phosphate Ion Adsorption at the Andosol Surface

Fraction	Ad-brut	FF(0-2µm)	ZV(0-20µm)
Quantity of phosphate adsorbed (mg/g)	3.08	1.74	1.06

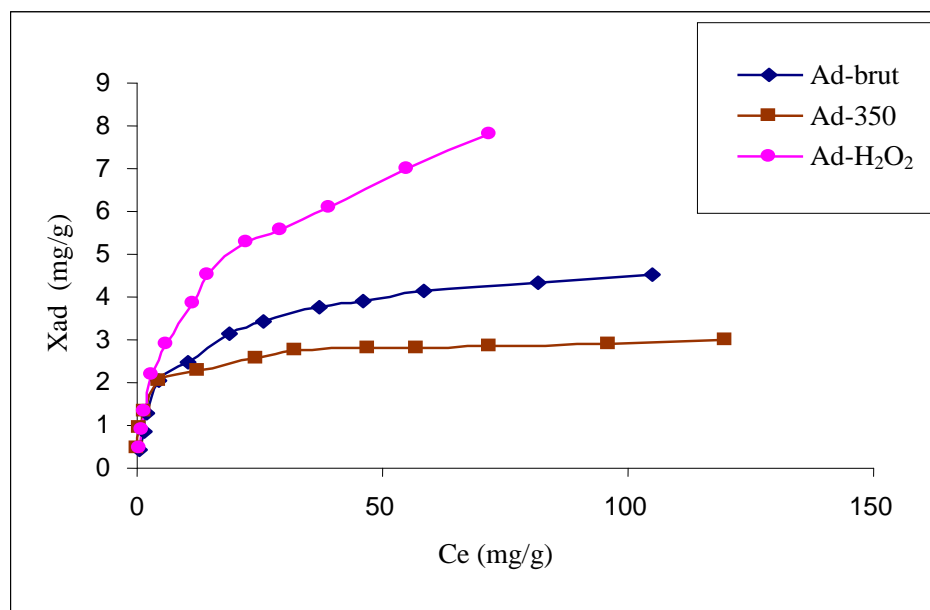


Fig. (7). Phosphate ions adsorption isotherms on each sample with the results fitted to the Langmuir equation.

ment at 350 °C (Ad-350). The results obtained are shown on Fig. (7).

These results show that the adsorption trend is as follows: Ad-H<sub>2</sub>O<sub>2</sub> > Ad-brut > Ad-350. The values of the coefficient of correlation R<sup>2</sup> confirm that the phosphate ion adsorption by the different samples is in agreement with the Langmuir model. The Langmuir parameters calculated and represented in Table 6 reveal that the maximum quantity adsorbed equals 4.75, 8.37 and 2.98 mg/g respectively for Ad-brut, Ad-H<sub>2</sub>O<sub>2</sub> and Ad-350. This result shows that the hydrogen peroxide pre-treatment helps to almost double the quantity of adsorbed phosphate ions relative to the raw andosol.

Hydrogen peroxide aqueous solution destroys the organic matter and liberates the amorphous minerals bearing hydroxyl functional groups, thus causing an increase in the number of ion adsorption sites. The works of Violante *et al.* [41] on phosphate adsorption have shown that there is competition between organic matter and orthophosphate anions on the adsorption sites. The organic matter removal therefore eliminates this competition leading to a high phosphate ions adsorption. On the contrary, the heating at 350 °C does not favour phosphate ion adsorption because thermal treatment apart from removing organic matter equally attacks the amorphous minerals. The thermal gravimetric curves of the raw andosols have shown a possible dehydration and dehydroxylation of amorphous minerals notably allophane between 100 and 183 °C [26]. Gibbsite dehydration occurs at about 320 °C: (2Al(OH)<sub>3</sub> → Al<sub>2</sub>O<sub>3</sub>+3H<sub>2</sub>O), while goethite

dehydration takes place from 320 °C (2FeO.OH → Fe<sub>2</sub>O<sub>3</sub> + H<sub>2</sub>O). Those minerals therefore lose their hydroxyl groups (S-OH) responsible for the fixing of phosphate anions [42, 8].

This study enables to understand that before combustion of organic matter that starts around 250 °C, thermal treatment has already destroyed the hydroxyl groups while hydrogen peroxide aqueous solution destroys the organic matter but does not affect the amorphous minerals present in andosols.

### 3.7.5. Effect of pH

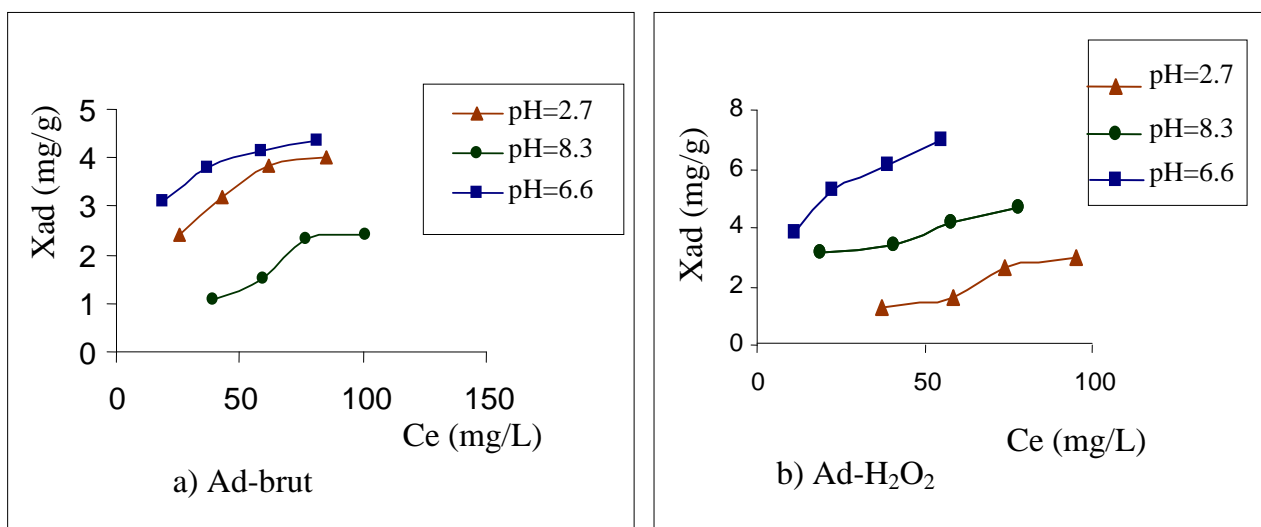
Three characteristic pH values of acid, neutral (distilled water) and basic media were tested; the quantity of phosphate adsorbed at equilibrium as a function of pH by Ad-brut and Ad-H<sub>2</sub>O<sub>2</sub> are shown by the curves Figs. (8a and 8b), respectively.

The raw andosol adsorbs more phosphate ions in the neutral medium (pH 6.6) than in the acidic (pH 2.7) and the basic (pH 8.3) media. Considering that it is the adsorption of negatively charged ionic species, the prediction theories might place the maximum adsorption in the acid medium because of the positively charged surface in the acid medium (S-OH + H<sup>+</sup> → S-OH<sub>2</sub><sup>+</sup>). This is verified at pH 2.7 while at pH 8.3, the surface of the andosol which bears a negative charge (S-OH + OH<sup>-</sup> → S-O<sup>-</sup> + H<sub>2</sub>O) [43] exercises an electrostatic repulsive influence on the phosphate ions. The slightly neutral medium (pH 6.6) is obtained with distilled

Table 6. Langmuir Parameters for each Sample

Samples	R <sup>2</sup>	K x 10 <sup>3</sup> (L/g)	Q <sub>max</sub> (mg/g)
Ad-brut	0.9971	128.60	4.751
Ad-H <sub>2</sub> O <sub>2</sub>	0.9818	95.73	8.368
Ad-350	0.9985	44.87	2.984





**Figs. (8a and b).** pH influence on phosphate ions adsorption over Ad-brut and Ad-H<sub>2</sub>O<sub>2</sub> samples.

water while the acid medium is obtained with an HCl acid solution; the slight prevalence of the neutral medium on the acid one can be explained by the competition between the chloride (introduced by the acid) and the phosphate ions on the raw andosol adsorption sites.

The H<sub>2</sub>O<sub>2</sub> treated andosol preferentially adsorbs phosphate ions at pH 6.6, then at 8.3 and finally at pH 2.7; there is an inversion of the general trend of results obtained between pH 2.7 and 8.3 relative to theoretical predictions of surface charges as previously explained. Hydrogen peroxide aqueous solution destroys the organic matter with an increase in the surface area for adsorption; but the introduction of the HCl so as to establish a pH of 2.7 instead destroys the aluminous octahedral sites (Al-O) [44] of the allophane. At pH 6.6, the maximum adsorption of phosphate ions (7.5 mg/g for Ad-H<sub>2</sub>O<sub>2</sub> against 4.5 mg/g for Ad-brut) is an evidence of an increase in the number of adsorption sites due to destruction of the allophane-humus complex followed by the elimination of organic matter.

In the acid medium, the comparison of the results obtained in Figs. (8a) and (8b) by the samples Ad-brut and Ad-H<sub>2</sub>O<sub>2</sub> respectively shows maxima of 4.02 and 3.00 mg/g of adsorbed phosphate ions. Ad-brut sample seems advisable for acid phosphate effluent treatment. In the basic medium, the maximum quantities of phosphate adsorbed are respectively equal to 2.32 and 4.68 mg/g for ad-H<sub>2</sub>O<sub>2</sub> and Ad-brut. The latter is better indicated for basic phosphate effluent treatment. The phosphate effluents at pH close to neutrality could be treated by Ad-H<sub>2</sub>O<sub>2</sub> which adsorbs 1.5 times more phosphate ions than Ad-brut.

#### 4. CONCLUSION

The andosols of the Bambouto mountains contain only about 9 % of fine clayey fraction, but close to 70 % of silty fraction. The amorphous minerals identified form complexes with organic matter present in the material. Hydrogen peroxide aqueous solution can thus be used to eliminate the organic matter without affecting the amorphous minerals which are the providers of hydroxyl functional groups responsible for the adsorption of phosphate ions. The kinetics

of adsorption of the phosphate ions is a chemisorption process which is carried out in two steps: a rapid step which ends approximately after two hours during which 67 % of phosphate ions is adsorbed and a slower step corresponding to 33 % of phosphate ions adsorption. The liberated allophane seems rather unstable in acid medium. The acid phosphate effluent can be treated by the raw andosol meanwhile the basic phosphate effluent can instead be treated with andosols whose organic matter has been removed using hydrogen peroxide solution. A water sample collected in the Yaounde Municipal Lake has 0.18 mg/l of phosphate ions at a pH of 6.03. This water could be freed of their phosphate ions contents with the raw andosol material from the Bambouto Mountains. The mass of andosol necessary to treat (within the laboratory conditions) one cubic meter of this water might be about 50 grams.

#### ACKNOWLEDGEMENTS

This work has been made possible by aid from Professor Olivier VITTORI from the "Laboratoire d'Electrochimie Analytique" of the "Université Claude-Bernard: Lyon 1/CPE Lyon"; Professor Emmanuel NGAMENI from the "Laboratoire de Chimie Analytique" of the University of Yaoundé 1; and Professor Robert CHAREYRON from the "Laboratoire d'Analyse Industrielle" of "Unité CPE Lyon, France". The authors hereby address special thanks to the above professors for their significant contributions.

#### REFERENCES

- [1] Fieldes, M. N.Z. *J. Sci. Technol.*, **1955**, B 37, 336-350.
- [2] Tardy, Y. *Pétrologie des latérites et des sols tropicaux*, Masson: Paris, **1993**.
- [3] Tematio, P.; Kengni, L.; Bitom, D.; Hodson, M.E.; Fopoussi, J.C.; Leumbe, O.; Mpakam, H.G.; Tsozué, D. *J. Afr. Earth Sci.*, **2004**, 39, 447-457.
- [4] Tématio, P. In *Thèse de Doct. d'Etat*; Univ. Yaoundé I, **2005**.
- [5] Diez, M. C.; Mora, M. L. and Videla, S. *Water Res.*, **1999**, 33, 1, 125-130.
- [6] Mora, M. L.; Canales, J. *Plant Anal.*, **1995**, 26, 17/18, 2805-2817.
- [7] Decarreau, A. *Matériaux argileux structure, propriétés et applications*, Société Française de Minéralogie et de Cristallographie: Paris, **1990**.
- [8] Shin, E. W.; Han, J. S.; Jang, J.; Min, S.H.; Kwang, P. J.; Rowell, R. M. *Environ. Sci. Technol.*, **2004**, 38, 912-917.

- [9] Hsu, P. H. *Soil. Sci. Soc. Am. Proc.*, **1964**, 28, 474.
- [10] Kuo, S.; Lotse, E.G. *Soil Sci. Soc. Am. Proc.*, **1974**, 38, 50-54.
- [11] Clark, C. J.; McBride, M. B. *Clays Clay Miner.*, **1984**, 32, 4, 291-299.
- [12] Xiang, Q.; Xie, H.Q.; Henderson, H.; Kay, A.F.; Fontes, M. P. F.; Weed, S. B. *Geoderma*, **1996**, 72, 37-51.
- [13] Ho, Y.S.; Chiang, C.C.; Hsu, Y.C. *Adsorption*, **2001**, 7, 139-147.
- [14] Banat, F.; Al-Asheh, S.; Al-Ahmad, R.; Bni-Khalid, F. *Bioresour. Technol.*, **2007**, 98, 3017-3025.
- [15] Dupain, R.; Lanchon, J. C.; Saint Arroman. *Granulals, sol, ciment et bétons. Caractérisation de matériaux de genie civil par les essais de laboratoire*. Casteilla: Paris, **2000**.
- [16] Ségalen, P. *Cahiers ORSTOM, sér. Pédol.*, **1968**, 6, n°1, 105-126.
- [17] Van Raij, B.V.; Peech, M. *Soil Sci. Soc. Am. Proc.*, **1972**, 36, 587-593.
- [18] Djoufac, W. E.; Djiogué, C.; Njopwouo, D. *Ann. Fac. Sci., Univ. YdéI, serie Maths-Info-phys. Chim.*, **1999**, 32, 125-135.
- [19] Rodier, J. *L'analyse de l'eau 7<sup>e</sup> edition*, Dunod: Paris, **1984**.
- [20] Fontès, M.P.F.; Weed, S.B. *Geoderma*, **1996**, 72, 37-51.
- [21] Adhikari, M.; Majundar, M.K.; Pati, A.K. *Fertilizer Technol.*, **1981**, 18, 71-74.
- [22] Sieffermann, G.; Jenl, G.; Rillot, G. *Bull. Argiles*, **1968**, 109-129.
- [23] Mackenzie, K. J. D.; Bowden, M. E.; Meinhold, R. H. *Clays Clay Miner.*, **1991**, 39, 4, 337-346.
- [24] Monteiro, S. N.; Viera, C.M.F. *Tile Brick Int.*, **2002**, 18, 3, 152-157.
- [25] Chinje Melo, U.F.; Kamseu, E.; Djangang, C. *Tile Brick Int.*, **2003**, 19, 6, 384-390.
- [26] Teruo, H. *Clays Clay Miner.*, **1980**, 28, 92-96.
- [27] Quantin, P. *Cah. ORSTOM, Sér. Pédol.*, **1972**, 10, n°3, 273-301.
- [28] Rollet, A.P.; Bouaziz, R. *L'analyse thermique tome 2*, Gauthiers-Villars: Paris, **1972**.
- [29] Bohn, H. L.; Mc Neal, B. L.; O'Cunnur, G.A. *Soil Chemistry*, Wiley: New York, **1979**.
- [30] Miranda-Trevino, J. C.; Coles, C. A. *Appl. Clay Sci.*, **2003**, 23, 133-139.
- [31] Egashira, K.; Aomine, S. *Clay Sci.*, **1974**, 4, 231-242.
- [32] Hashizume, H.; Theng, B. K. G. *Clay Miner.*, **1999**, 34, 233-238.
- [33] Jarvinen, E.; Hokkanen, T. j.; Kuuluvainen, T. *Scand. J. For. Res.*, **1993**, 8, 435-445.
- [34] Chiou, C. T. Lee, J. F. Boyd, S. A. *Environ. Sci. Technol.*, **1990**, 24, 1164-1166.
- [35] Churchman, G. J.; Burke, C. M. *J. Soil Sci.*, **1991**, 42(3) 463-478.
- [36] Madeira, M.; Auxtero, E.; Sousa, E. *Geoderma*, **2003**, 117, 225-241.
- [37] Karlun, E.; Bain, D.C.; Gustafsson, J.P.; Mannerkoski, H.; Murad, E.; Wagner, U.; Fraser, A.R.; Mchardy, W.J.; Starr, M. *Geoderma*, **2000**, 94, 265-288.
- [38] Giles, C.H., Smith, D.; Huitson, A. *J. Colloid Interf. Sci.*, **1974**, 47, 755-765.
- [39] Torrent, J. *Soil Sci. Soc. Am. J.*, **1987**, 51, 78-82.
- [40] Barrow, N.J. Proceedings of phosphorus requirements for sustainable agriculture in Asia and Oceania, March **1989**.
- [41] Violante, A.; Gianfreda, L. *Soil Sci. Soc. Am. J.*, **1993**, 57, 1235-1241.
- [42] Goldberg, S.; Sposito, G. *Commun. Soil Sci. Plant Anal.*, **1985**, 16, 801-821.
- [43] Illès, E.; Tombacz, E. *J. Colloid Interf. Sci.*, **2006**, 295(1), 108-114.
- [44] Wada, K. *Am. Mineral.*, **1967**, 52, 690-708.

Received: April 16, 2008

Revised: July 16, 2008

Accepted: July 16, 2008

© Siéwé et al.; Licensee Bentham Open.

This is an open access article licensed under the terms of the Creative Commons Attribution Non-Commercial License (<http://creativecommons.org/licenses/by-nc/3.0/>) which permits unrestricted, non-commercial use, distribution and reproduction in any medium, provided the work is properly cited.